Catalysis Science & Technology

Accepted Manuscript

ROYAL SOCIETY OF CHEMISTRY

www.rsc.org/catalysis

Journal Name

RSCPublishing

ARTICLE

Gas-phase oxidation of ethanol over Au/TiO_2 catalysts to probe metal-support interactions

Cite this: DOI: 10.1039/xoxxoooooox

M.C. Holz[a], K. Tölle[a], and M. Muhler[a],

Received ooth January 2012,
Accepted ooth January 2012

DOI: 10.1039/xoxxoooooox

www.rsc.org/

Ethanol and oxygen were converted over titania and gold nanoparticles supported on titania to investigate the reactivity of the support, the influence of the metal, and the role of metal-support interactions. In addition to determining the degrees of conversion and the yields as a function of temperature, temperature-programmed desorption and diffuse reflectance infrared spectroscopy were applied in fixed-bed reactors under continuous flow conditions. Over pure TiO_2 mainly selective oxidative dehydrogenation to acetaldehyde and water and, to a minor extent, total oxidation to CO_2 and H_2O were found to occur above 500 K. The presence of Au nanoparticles additionally induced the selective oxidation to acetaldehyde and H_2O at temperatures below 400 K. Thus, the Au/TiO_2 catalyst shows bifunctional properties in oxygen activation needed for the selective oxidation of ethanol. Ethoxy species were detected by IR spectroscopy, which are identified as intermediate species in ethanol conversion. In contrast, strongly bound acetates and acetic acid acted as catalyst poison for the selective low-temperature oxidation route, but not for the high-temperature route. Selective low-temperature oxidation is assumed to occur at the perimeter of the Au nanoparticles, which additionally enhance the high-temperature oxidation route on TiO_2 pointing to a Mars–van Krevelen mechanism based on an enhanced reducibility of TiO_2.

Introduction

In recent years hydrogen production from hydrogen-rich molecules became a topic of growing interest due to its possible application in fuel cells.[1–3] Many studies focus on the catalytic production of hydrogen from ethanol via steam reforming[4–6] or partial oxidation[7–10] over several types of catalysts, but the mechanisms of both reactions are still under discussion. Especially the oxidation of alcohols is a key technology in industry as selective products like aldehydes or ketones are widely used in industrial organic synthesis.[11–13] Therefore, mechanistic studies may provide the basis to further improve catalyst activity and selectivity.

Oxidation of ethanol (eq. 1) is one of the oldest methods used to produce acetaldehyde commercially catalyzed by Cu- or Ag-based catalysts:[13]

(1) $2\ CH_3CH_2OH + O_2 \rightarrow 2\ CH_3CHO + 2\ H_2O$

In general, acetaldehyde is reported as main selective oxidation product.[6,7,9,10,14–16] Additionally, ethene, water, hydrogen, carbon monoxide, carbon dioxide, methane, and traces of acetic acid, diethyl ether, and ethyl acetate were detected.[9,10]

Recently, Murzin and co-workers[17–19] studied ethanol oxidation over differently loaded Au/TiO_2 catalysts. While for the pure support material conversion of ethanol starts to increase at about 413 K, the authors observed a "double-peak" catalytic activity for the reaction over Au/TiO_2. A low-temperature maximum at 393 K and a high-temperature maximum above 473 K in the conversion of ethanol as well as in the selectivity of the main oxidation product acetaldehyde were reported.[17–19] The conversion and selectivity profiles in the high-temperature region are similar to the conversion profile detected over pure TiO_2. However, for TiO_2 mainly acid-base catalyzed reactions to diethyl ether (eq. 2) and ethene (eq. 3) rather than the formation of acetaldehyde were observed.[18]

The formation of additional products such as 1,1-diethoxyethane, acetic acid, ethyl acetate, diethyl ether, or ethene over Au/TiO_2 was found to occur to a minor extent.[17]

(2) $2\ CH_3CH_2OH \rightarrow (CH_3CH_2)_2O + H_2O$

(3) $CH_3CH_2OH \rightarrow C_2H_4 + H_2O$

The comparison of Au/TiO_2 with Au/Al_2O_3 and Au/SiO_2 revealed that the observed low-temperature activity of catalysts with an Au loading of 2–7 wt% is quite unusual in gold catalysis.[18] The authors propose the formation of a specific active oxygen species at the catalytic sites on Au/TiO_2 being responsible for the low-temperature activity at 393 K. The generation of the active oxygen species is assumed to be possible under mild conditions in the presence of hydrogen.[19]

Surface O^- anion radicals, surface O_2^- superoxide anions, or peroxides are suggested as active species at low temperatures.[19] The sharp drop in activity is assumed to be due to the decomposition, desorption, or suppressed production of the highly active oxygen species at higher temperatures.[17,19] Strong deactivation due to the deposition of organic species on the catalyst surface via coking was supposed as well, as the initial catalytic activity was restored after an additional oxidative pre-treatment.[17] Even though oxygen is assumed to be needed as intrinsic promoter of the dehydrogenation reaction the conversion of ethanol follows the non-oxidative pathway (eq. 4) at high temperatures.[18] Similarly, catalyst deactivation due to coking was also observed by Carotenuto et al.[7] during ethanol dehydrogenation over copper-chromite and copper-zinc catalysts supported on alumina. The use of a relatively low amount of oxygen was found to be necessary to reduce coke formation.[7]

(4) $CH_3CH_2OH \rightarrow CH_3CHO + H_2$

Studies performed over octahedral molecular sieve catalysts (OMS-2) focused on the role of lattice oxygen and Lewis acid sites in ethanol oxidation.[9] Acetaldehyde was identified as major intermediate, but also the formation of formaldehyde, acetic acid and total oxidation of all intermediates to CO_2 and H_2O was observed. Acetaldehyde and formaldehyde are also produced in absence of O_2 in the feed gas due to oxidation by lattice oxygen. In presence of O_2 this reaction pathway is followed by total oxidation of all species including ethanol, acetaldehyde, formaldehyde, and acetic acid to CO_2.[9] The lattice oxygen vacancies are re-filled by O_2 from the gas-phase pointing to a Mars-van Krevelen mechanism. More precisely, ethanol adsorbs on a Lewis acid site and oxidation takes place with lattice oxygen serving as basic site. Then, the Lewis acid sites are re-oxidized via replenishment of lattice oxygen.[9] The authors observed also deactivation phenomena during reaction due to competitive adsorption of water vapor and ethanol on the active sites of the catalyst suppressing the acetaldehyde formation.[9] A similar reaction mechanism was observed by Iglesia and co-workers[20] for ethanol oxidation over vanadium oxide domains supported on γ-Al_2O_3. Lattice oxygen was identified to be required for ethanol oxidation to acetaldehyde.[20] Temperature-programmed desorption (TPD) and surface reaction (TPSR) studies over MnO_x-CeO_2 mixed oxides support the idea of a Mars-van Krevelen mechanism proceeding during ethanol oxidation.[10] TPD profiles confirm the low-temperature oxidative dehydrogenation towards acetaldehyde via interaction with lattice oxygen, as coincident H_2O formation was detected at about 405 K.

In situ FTIR studies using ethanol as surface probe and as reactant for ethanol oxidation or steam reforming were performed in order to identify adsorbed intermediates as well as the mechanism of the oxidation reaction under reaction conditions.[4–10,15,21,22] Similar to methanol adsorption on TiO_2-based catalysts ethanol adsorbs mainly dissociatively on the TiO_2 surface, resulting in mono- and bidentate adsorption of ethoxy species.[5,21] In addition to bands related to ethoxy species, bands assigned to molecularly adsorbed ethanol are identified.[5,15,21,22] During evacuation at 423 K physically adsorbed ethanol is removed from the surface.[15] Increasing the temperature leads to decomposition of the irreversibly adsorbed ethoxy species forming adsorbed acetates and acetaldehyde in the gas phase at about 523 K. Further heating results in decomposition of the adsorbed acetate species at 673 K producing CO_2 and small amounts of CO. H_2O is formed continuously throughout the heating process accompanied by the formation of gas-phase ethene.[15] TPD studies performed in a FTIR spectrometer supported the observed formation of ethene, acetaldehyde, ethane, methane, CO_2, H_2O, and H_2 during ethanol decomposition accompanied by desorption of molecular ethanol.[5]

It is the aim of this study to gain deeper insight into the mechanism of ethanol oxidation over Au/TiO_2 addressing the influence of the Au particles, the TiO_2 support, and the metal-support interactions. Furthermore, the different adsorbates are identified and their role in the ethanol oxidation reaction is assessed by performing transient kinetic experiments and by applying infrared spectroscopy under continuous flow conditions in fixed-bed reactors.

Experimental Section

An all stainless-steel microreactor set-up with a calibrated quadrupole mass spectrometer (QMS, Balzers GAM422) was used for the oxidation of ethanol. A detailed description of the set-up is given in Ref.[26] Shortly, the microreactor consisted of a glass-lined stainless steel U-tube with an inner diameter of 4 mm, which was heated in an aluminum block oven. For catalytic tests the U-tube reactor was filled with 100 mg of the sample (250 – 355 µm). A commercially available 1.1 wt% Au/TiO_2 catalyst AURO*lite*™ (*STREM Chemicals*) and the support material TiO_2 (P25, *Degussa/Evonik*), were tested. The sample was diluted with 100 mg of glass beads, except for the TPD experiments. A thermocouple was directly placed in the catalyst bed. Time-resolved quantitative online gas analysis was performed with a calibrated QMS. Dosing of ethanol was achieved by purging a saturator with He (99.9999% purity). The vessels were cooled by means of a cryostat to 273 K, resulting in a saturated mixture of 1.575% ethanol in He. By means of mixing valves ethanol/He and O_2 were mixed and further diluted by He. Thus, an initial feed of 3900 ppm ethanol and 3900 ppm O_2 in He was provided for the oxidation experiments. All gas flows were adjusted by calibrated mass flow controllers (MFCs).

The FTIR studies were performed using a Nicolet Nexus FTIR spectrometer with a liquid nitrogen-cooled mercury cadmium telluride (MCT) detector. A Nicolet environmental cell with ZnSe windows was used, and a spectral resolution of 4 cm^{-1} was chosen for all measurements.

Ethanol temperature-programmed desorption (TPD) experiments were performed after pre-treatment in 10% O_2/He (10 sccm) at 723 K for 4 h. After cooling to 300 K and purging

of the reactor with He the sample was exposed to 1.575% CH_3CH_2OH in He (10 sccm) until saturation was reached. Subsequently the reactor was purged with He for 60 min to remove the ethanol and then heated to 723 K with a heating rate of 3 K min^{-1}.

The catalysts used in ethanol decomposition and ethanol oxidation activity tests were pre-treated similarly in 10% O_2/He (10 sccm) for 4h at a maximum temperature of 573 K. After cooling to 300 K the ethanol decomposition or oxidation experiments were performed. For ethanol decomposition a 0.39% CH_3CH_2OH/He reaction gas was passed over the catalyst (100 sccm) and the sample was heated to 573 K with a heating ramp of 0.5 K min^{-1}. The temperature was kept constant for 1 h before the sample was cooled to room temperature with 0.5 K min^{-1}. For ethanol oxidation the procedure was similar, but the feed gas composition was changed to 0.39% CH_3CH_2OH/0.39% O_2/He. The ethanol oxidation experiment was repeated directly without any further pre-treatment.

The ethanol oxidation was also studied in the IR cell over Au/TiO_2 after an oxidative pre-treatment. The gas flow was decreased to 30 sccm with the same reactant concentrations as mentioned above. The heating rate was changed to 1 K min^{-1}. At the maximum temperature of 573 K the reaction gas was switched to He for 30 min followed by a switch to 0.39% O_2/He for 30 min studying the mobility of the adsorbed surface species. The spectra were recorded against KBr as background. The KBr background was recorded independently at different temperatures. During heating series measurements (100 scans) were performed with a change of the KBr background spectra every 25 K.

Results and Discussion

Ethanol TPD

Exposure of TiO_2 and Au/TiO_2 to ethanol at 303 K resulted in an uptake of 337 and 342 µmol/g_{cat}, respectively, derived from the breakthrough curves. Ethanol is known to adsorb molecularly and dissociatively on metal oxide surfaces.[4–10,15,20–25] Thus, it can be assumed that ethanol adsorbs on the exposed TiO_2 surfaces. The QMS traces of the subsequent TPD experiments with a heating rate of 3 K min^{-1} are shown in Figure 1 for both catalysts. For both samples small amounts of molecularly adsorbed ethanol were detected to desorb below 575 K.

(Insert Figure 1 here)

Figure 1. QMS traces of the ethanol TPD experiments with A) TiO_2 and B) Au/TiO_2 displaying the effluent mole fractions of CH_3CH_2OH (—), H_2O (— — —), $CH_2{=}CH_2$ (—), CH_3CHO (▪▪▪), H_2 (□ ▪ ▪), $(C_2H_5)_2O$ (— — —), and CO_2 (▪▪▪). The heating rate was 3 K min^{-1}.

For pure TiO_2 (Figure 1 A) desorption of ethanol occurred over a very broad temperature range (315 to 575 K) whereas the ethanol desorption signal is rather narrow for Au/TiO_2 (Figure 1 B). From the latter ethanol desorbed mainly around 359 K. For TiO_2 (Figure 1 A) simultaneous desorption of H_2O and ethene started at about 325 K. The QMS trace of H_2O shows two desorption maxima at 461 and 570 K. The high-temperature desorption maximum of water is accompanied by the desorption of ethene with a maximum at 583 K clearly indicating the dehydration of adsorbed ethoxy species. In addition, traces of desorbing diethyl ether around 550 K and small amounts of simultaneous desorbing acetaldehyde (570 K) and H_2 (564 K) indicating dehydrogenation of adsorbed ethoxy species were detected. For the Au/TiO_2 sample (Figure 1 B) only negligible amounts of ethene desorbed between 325 and 525 K coincident with the desorption of H_2O (maximum at 484 K). In addition to the desorption of molecular ethanol only small amounts of ethene and acetaldehyde were observed as carbon-containing species desorbing below 500 K. The formation of CO_2 was detected only above 575 K. Hydrogen was detected as main desorption product with desorption maxima at 490 and 657 K and a shoulder peak at 612 K. The results indicate that the dehydrogenation is strongly favoured in the presence of the Au nanoparticles on TiO_2. The total amounts of desorbing species are summarized in Table 1.

Table 1. Amounts of desorbing species detected during the temperature-programmed desorption (TPD) experiments with 3 K min^{-1} subsequent to ethanol exposure at 303 K.

	n_{des} [µmol/g_{cat}]	
species	TiO_2	Au/TiO_2
CH_3CH_2OH	104	39
$CH_2{=}CH_2$	94	24
CH_3CHO	30	18
$(C_2H_5)_2O$	14	0
H_2O	184	175
H_2	22	295
CO_2	0	25

For pure TiO_2 the mass balances for carbon (76%) and hydrogen (83%) are almost closed. Even though a small amount of adsorbed ethanol remains on the catalyst surface the ratio of the total amounts of carbon and hydrogen atoms in desorbing species is nearly 1:3 as expected. Therefore, most of the adsorbed ethanol decomposes mainly to ethene and H_2O as well as acetaldehyde and H_2 during the TPD experiment accompanied by the formation of traces of diethyl ether.

For the Au/TiO_2 catalyst the mass balances cannot be closed. The ratio of the total amounts of desorbing carbon and hydrogen atoms is 1:7. This observation indicates that carbon- and hydrogen-containing species remain on the surface even at temperatures as high as 723 K, which is supported by a change

of the colour of the samples after the experiment from violet to brown.

Ethanol conversion in the absence of O_2

The results of the ethanol decomposition experiments over TiO_2 and Au/TiO_2 are shown in Figure 2. The reported yields refer to the initial amount of ethanol. Conversion of ethanol over pure TiO_2 starts at 500 K and at maximum reaction temperature maximum conversion of ethanol (37%) is achieved. Simultaneous formation of acetaldehyde and H_2 (1:1) and simultaneous formation of ethene or diethyl ether and H_2O was observed at temperatures between 500 and 573 K.

((Insert Figure 2 here.))

Figure 2. Conversion and yields during ethanol decomposition over (A) TiO_2 and (B) Au/TiO_2 after O_2 pre-treatment at 573 K. Conversion of CH_3CH_2OH (◀) and yields of H_2 (▲, □), H_2O (●, □), CH_3CHO (♦, □), $CH_2{=}CH_2$ (▼, □), and $(C_2H_5)_2O$ (▶, □) are shown. Traces with full symbols were obtained during heating, traces with open symbols during cooling of the catalyst.

The conversion of ethanol and the product yields detected during heating and cooling do not differ significantly. Thus, steady-state conditions were nearly achieved during ethanol decomposition over bare TiO_2. Over the Au/TiO_2 catalyst the conversion of ethanol starts already at 425 K. At the maximum temperature much more ethanol is consumed (75%) than over bare TiO_2. As was observed for TiO_2, the simultaneous formation of acetaldehyde and H_2 starts concurrently with the conversion of ethanol, but at lower temperatures (425 K). Up to about 525 K a 1:1 formation of acetaldehyde and H_2 can be observed as expected (eq. 4), but above this temperature more H_2 than acetaldehyde is formed. Even though the formation of H_2O is detected at temperatures above 450 K only traces of ethene and negligible formation of diethyl ether were observed. During cooling the conversion of ethanol and all detected product yields differ significantly from the data detected during heating, i.e., they are shifted to higher temperatures. This observation indicates that steady-state conditions were not achieved during ethanol decomposition over Au/TiO_2.

The results of the TPD experiments indicate that carbon- and hydrogen-containing species remain on the surface of the Au/TiO_2 catalyst as the mass balance was not closed. Acetic acid formation leading to strongly adsorbed species may be a reasonable explanation. The comparison of the ion currents of all C_2-compounds reveals that only negligible traces of acetic acid are formed during the decomposition reaction. Therefore, the challenging calibration of the QMS for acetic acid was not performed even though traces of acetic acid are formed.

In summary, dehydrogenation to acetaldehyde and hydrogen and dehydration to ethene or diethyl ether and H_2O are the main reaction pathways observed during ethanol decomposition over TiO_2 and Au/TiO_2. In to the presence of Au nanoparticles on TiO_2 ethanol conversion is enhanced significantly, and ethanol conversion and concurrent dehydration to acetaldehyde start at lower temperatures compared with pure TiO_2. The conversion and yields detected during heating and cooling over Au/TiO_2 differ significantly, presumably due to catalyst deactivation as was also observed for methanol and 2-propanol oxidation.[23,26] In this regard acetic acid or other adsorbed intermediates of the ethanol oxidation are likely poisoning species. Especially, acetic acid is known to adsorb strongly on the catalyst surface, which has already been suggested by Li et al.[10] Therefore, the catalysts surface and the adsorbed intermediate species were further studied by means of IR measurements.

Ethanol oxidation

The conversion of ethanol and O_2 over TiO_2 with a feed gas of 0.39% CH_3CH_2OH/ 0.39% O_2/He is shown in Figure 3 in the temperature range between 303 and 573 K indicating considerable activity for ethanol oxidation at temperatures above 500 K. At maximum reaction temperature (573 K) about 50% conversion of ethanol and 30% conversion of O_2 are achieved. The main products were acetaldehyde and H_2O. Additionally, traces of carbon dioxide were detected. The reported yields refer to the initial amount of ethanol. Taking into account eq. 1 a 1:1 formation of acetaldehyde and H_2O would be expected, but less water than acetaldehyde is observed in the gas phase, even though additional formation of CO_2 starts at about 550 K. Based on these observations it is reasonable to assume that total oxidation as well as selective oxidation to acetaldehyde and water take place, but water seems to remain partially on the catalyst surface. During cooling almost similar degrees of conversion and yields of all compounds observed during heating are detected, i.e. steady state was nearly achieved.

((Insert Figure 3 here.))

Figure 3. Conversion and yields during ethanol oxidation over TiO_2 after O_2 pre-treatment at 573 K. Conversion of CH_3CH_2OH (◀, □) and O_2 (★, □) and yields of H_2O (●, □), CO_2 (■, □), and CH_3CHO (♦, □) are shown. Traces with full symbols were obtained during heating, traces with open symbols during cooling of the catalyst.

The presence of Au nanoparticles (1.1 wt%) on TiO_2 resulted in a very active catalyst for ethanol oxidation. The catalyst was active for ethanol conversion after oxidative pre-treatment already in the low-temperature region as shown in Figure 4 A. The conversion of ethanol and O_2 started immediately after initiation of the heating ramp of 0.5 K min^{-1} at 303 K.

((Insert Figure 4 here.))

Figure 4. Conversion and yields during ethanol oxidation over Au/TiO_2 after O_2 pre-treatment at 573 K (A: 1st run, B: 2nd run). Conversion of CH_3CH_2OH (◀, □) and O_2 (★, □) and yields of H_2O (●, □), CO_2 (■, □), and CH_3CHO (♦, □) are shown. Traces with full symbols are obtained during heating, traces with open symbols during cooling of the catalyst.

In contrast to pure TiO_2, a first maximum in the conversion of ethanol (13%) was observed already at T = 358 K during the first heating paralleled by a first maximum in the yield of acetaldehyde (11%). The formation of acetaldehyde is accompanied by the formation of traces of H_2O. Increasing the temperature beyond this point resulted in a sustained conversion of ethanol and conversion of O_2 starting at about 450 K. Contrary to eq. 1 the formation of acetaldehyde and water differs from a 1:1 ratio, even though the ratio of ethanol and oxygen conversion is nearly 2:1. At about 525 K also the formation of CO_2 is observed. The maximum yields of acetaldehyde (55%), H_2O (26%), and CO_2 (9%) were achieved at the highest reaction temperature. During cooling the conversion of ethanol and O_2 as well as the yield of acetaldehyde differ significantly in the low-temperature region from those detected during heating. Similar to ethanol decomposition only traces of acetic acid were formed during the oxidation reaction. In a second experiment without additional oxidative pre-treatment the first maximum in acetaldehyde formation is not observed (Figure 4 B). The heating and cooling branches coincide with those recorded during cooling in the first run. The decrease in conversion may indicate the consumption of a highly active species during the initial heating as proposed for ethanol oxidation over Au/TiO_2,[18,19,35] or it may result from poisoning of the catalyst during the first reaction cycle as observed in methanol or 2-propanol oxidation over Au/TiO_2.[23,26] The low-temperature activity can be restored by additional oxygen pre-treatment (not shown).

This issue was studied further by means of IR spectroscopy. Figure 5 shows the *in situ* DRIFT spectra of the Au/TiO_2 catalyst during ethanol oxidation after oxidative pre-treatment at 573 K. Bands at 3675 and 3630 cm^{-1} assigned to bridging $(Ti)_2OH$ species[27] and a very broad band centered at 3442 cm^{-1} related to surface OH groups are observed after the catalyst pre-treatment (Figure 5, spectrum a). An additional band at 1622 cm^{-1} is observed, which might be due to OH bending vibration of molecular water ($\delta(H_2O)$).[27,28] After exposure of the catalyst to a 0.39% CH_3CH_2OH/0.39% O_2/He reaction gas mixture, all bands assigned to surface OH groups decrease significantly or disappear completely.

((Insert Figure 5 here.))

Figure 5. DRIFT spectra detected during ethanol oxidation over of Au/TiO_2 after oxidative pre-treatment: (a) at 303 K in He after pre-treatment in O_2/He at 573 K; in 0.39% CH_3CH_2OH/ 0.39% O_2/ He at (b) 303 K, (c) 373 K, (d) 423 K, (e) 523 K, and (f) 573 K.

Now, they contribute to a broad, H-bonded ν(OH) between 3600 and 3000 cm^{-1} leading to a sharper superimposed absorption at 3407 cm^{-1}. This band can be assigned to ν(OH) of an undissociated adsorbed ethanol molecule and is accompanied by a band at 1398 cm^{-1} due to asymmetric CH_3 stretching vibrations $\delta_a(CH_3)$[21] and a small band due to δ(OH) at 1260 cm^{-1}.[5,15,21] Additional bands at 2973, 2930, 2901, 2871, 1473, 1448, 1378, 1356, 1135, 1074, 1066, and 1049 cm^{-1} appear indicating dissociative adsorption of ethanol yielding ethoxy species, which is the main adsorption pathway on Au/TiO_2. The bands are assigned to the asymmetric CH_3 and CH_2 stretching vibrations ($\nu_a(CH_3)$: 2973 cm^{-1}; $\nu_a(CH_2)$: 2930 cm^{-1}), the symmetric CH_3 and CH_2 stretching vibrations ($\nu_s(CH_2)$: 2901 cm^{-1}; $\nu_s(CH_3)$: 2871 cm^{-1}), the scissoring CH_2 vibration (sci(CH_2); 1473 cm^{-1}), the asymmetric CH_3 bendings (($\delta_a(CH_3)$; 1448 cm^{-1}), the symmetric CH_3 bendings ($\delta_s(CH_3)$; 1378 cm^{-1}), the wagging CH_2 vibration ($\delta_{wag}(CH_2)$; 1356 cm^{-1}), the C-O stretching vibration of monodentate ethoxy adsorbed on a single Ti^{4+} site (ν(C-O): 1135 cm^{-1}), the C-C ((ν(CC), 1074, 1066 cm^{-1}), and the C-O stretching vibration of bridged bidentate ethoxy adsorbed on adjacent Ti^{4+} sites (ν(C-O): 1049 cm^{-1}).[5,15,21]

The bands assigned to ethoxy species decrease with increasing temperature indicating the consumption of those species. At temperatures between 373 and 523 K new bands at 1530, 1435, 1408, and 1393 cm^{-1} appear progressively. The bands at 1530 and 1435 cm^{-1} are due to the asymmetric and symmetric COO stretching vibrations of adsorbed acetates on TiO_2 ($\nu_a(COO)$, $\nu_s(COO)$), respectively.[15,29]

Wu et al.[21] and Ovari and Solymosi[22] assigned bands in the region of 1447 - 1440 cm^{-1} to asymmetric CH_3 bendings of adsorbed ethoxy species. However, it has to be noted that bands due to carbonate species were reported to occur in this region.[30] Usually, bands between 1406 and 1391 cm^{-1} are assigned to CH bendings (δ(CH)) or γ(OCO) vibrations of formate species ($HCOO^-$) adsorbed on TiO_2.[31–33] The bands assigned to molecularly adsorbed ethanol were observable up to 523 K. At higher temperatures the broad band in the region 3600 – 3000 cm^{-1} vanishes and only a small band centered at 3413 cm^{-1} is left. Due to the online product gas analysis it was found that the formation of water occurs over the whole temperature range (not shown). Therefore, the band at 3413 cm^{-1} may be due to surface OH on TiO_2, but also traces of molecularly adsorbed ethanol are reasonable. Additionally, bands at 3058 and 3014 cm^{-1} arise. Rachmady and Vannice[29] assigned a band at 3023 cm^{-1} to ν(CH) of crotonaldehyde and a band at 3016 cm^{-1} to $\nu(CH_3)$ of acetic acid adsorbed on Pt/TiO_2. Only traces of acetic acid were observed in the gas phase by QMS. Hence, it seems reasonable to assign the band at 3014 cm^{-1} to adsorbed acetic acid. Furthermore, a new small band occurs at 1699 cm^{-1}, which was assigned to adsorbed acetaldehyde on TiO_2 by Raskó et al.[5] The assignment to acetaldehyde is supported by its formation observed over the whole temperature range by means of QMS analysis (not shown). A new band at 2349 cm^{-1} is present at 473 K due to the formation of gas-phase CO_2 starting at about 460 K. At the maximum temperature of 573 K bands assigned to ethoxy species, acetate species, acetaldehyde, acetic acid, and presumably carbonate species are present on the surface.

After ethanol oxidation was performed in the IR spectrometer the reaction gas was switched to He at the maximum reaction temperature and after 30 min further changed to 0.39% O_2/He.

The results are shown in Figure 6. When the reaction gas is switched to pure He bands related to ethoxy species decrease slightly, while those assigned to gas-phase CO_2 disappear completely after 30 min. In contrast, the bands assigned to acetate species and adsorbed acetic acid seem to remain stable, while the one assigned to adsorbed acetaldehyde seems to increase slightly and shifts to higher wavenumbers (1706 cm^{-1}). Furthermore, new bands arise. The band located at 3639 cm^{-1} is presumably due to surface OH species on TiO_2. Three new bands occurring at 1691 (ν(C=O)), 1591 (ν(OCO)), and 1564 cm^{-1} are most likely due to formation of formates as observed in literature.[5,21,31,33] They are difficult to distinguish, because they are superimposed by other bands, e.g. the one located at 1530 cm^{-1} assigned to acetates. Thus, the bands assigned to formate species may be present before as well. Switching the feed gas to 0.39% O_2/He leads to an additional decrease of bands assigned to ethoxy species and the band located at 3413 cm^{-1} indicating the consumption of ethoxy species. Those bands assigned to adsorbed acetaldehyde seem to increase slightly, while adsorbed acetic acid, acetate species, and formate species seem to remain stable. Additionally, formation of gas-phase CO_2 starts again (2349 cm^{-1}) when the O_2/He gas mixture passes through the IR cell. A new band most likely due to adsorbed acetaldehyde seems to arise at about 1722 cm^{-1} after 29 min of exposure to 0.39% O_2/He.[5]

((Insert Figure 6 here.))

Figure 6. DRIFT spectra of Au/TiO_2: (f) in 0.39% CH_3CH_2OH/ 0.39% O_2/ He at 573 K, in He at 573 K for (g) 1 min, (h) 5 min, (i) 29 min, and in 0.39% O_2/ He for (j) 1 min, (k) 5 min, and (l) 29 min.

Discussion

The pure TiO_2 support showed considerable activity in the ethanol conversion experiments contrary to methanol oxidation.[26] In the high-temperature region oxidation of ethanol to acetaldehyde presumably due to oxidative dehydrogenation[10] can be observed. To a lower extent total oxidation to CO_2 was detected at about 550 K. Contrary to the results of Murzin and co-workers[17–19] no acid-base catalyzed reactions to diethyl ether and ethene occurred. Those products were only formed in the TPD and the ethanol decomposition experiments. During the TPD experiments the acid-base catalyzed dehydration to ethene was observed rather than dehydration to diethyl ether or dehydrogenation to acetaldehyde. In the ethanol decomposition experiment dehydrogenation to acetaldehyde and dehydration to ethene or diethyl ether were observed to a comparable extent, presumably acid-base catalyzed. In the oxygen-free experiments the partial oxidation products acetaldehyde and H_2O were both observed at high temperatures. Even though the results indicate that acetaldehyde is mainly due to dehydrogenation it may be possible that also partial oxidation to acetaldehyde and H_2O occurs as was reported by Li et al.[9] According to the authors the oxidation reaction at high temperatures follows a Mars-van Krevelen mechanism. It seems reasonable to assume that this reaction takes place also in the oxygen-free experiments, but only to a minor extent because of the limited supply of lattice oxygen. During ethanol oxidation the oxygen vacancies are re-filled directly by the gas-phase oxygen and the reaction can proceed following a Mars-van Krevelen mechanism. During cooling similar degrees of conversion and yields were detected in the co-feeding experiment as well as in the ethanol decomposition pointing to steady-state conditions.

The presence of Au nanoparticles (1.1 wt%) on TiO_2 results in a very active catalyst in ethanol oxidation already at low temperatures. At 358 K a first maximum in the selective conversion of ethanol (14%) and O_2 (6%) to acetaldehyde was detected accompanied by the formation of traces of H_2O. Even though the ratio of the reactants is nearly 2:1 as expected according to eq. 1, less H_2O than acetaldehyde is observed in the gas phase, presumably remaining on the catalyst surface. The low-temperature reaction only proceeds in presence of Au nanoparticles on TiO_2, but is not observed during ethanol decomposition over Au/TiO_2. Murzin and co-workers[17–19] studied ethanol oxidation over TiO_2 and differently loaded Au/TiO_2 catalysts and proposed the formation of a specific active oxygen species on the catalytic sites on Au/TiO_2 being responsible for the outstanding low-temperature activity. Accordingly, this active oxygen species is generated under mild conditions.[19] Similar to these results low-temperature activity is only observed in the co-feeding experiment over the Au-loaded catalysts. Farnesi Camellone et al.[34] reported that the activation of molecular oxygen for methanol oxidation occurs at the interface of Au and TiO_2 through charge transfer from Au/TiO_2 forming $O_2^{\delta-}$ species. It is reasonable to assume the formation of such active oxygen species for the selective low-temperature oxidation of ethanol. A large number of Au perimeter atoms correlates with activity in the low-temperature reaction. Thus, the oxygen activation under mild conditions is assumed to occur at the Au nanoparticles, presumably at the Au perimeter (active sites type I) as has already been proposed in the literature.[23,26]

In the high-temperature region the conversion of ethanol with O_2 results in the formation of acetaldehyde, H_2O, and CO_2 over Au/TiO_2. The simultaneous formation of acetaldehyde and H_2O is due to the oxidative dehydrogenation of ethanol, even though less H_2O than expected is formed. This may be explained by water remaining adsorbed on the catalyst surface in form of OH groups as indicated by the detected band at 3413 cm^{-1}, which can be most likely assigned to OH groups on TiO_2. In contrast to the low-temperature oxidation proceeding presumably at the perimeter of the Au nanoparticles (active sites type I), this reaction at higher temperatures seems to occur at active sites on TiO_2 (type II), because a similar behavior was observed during ethanol oxidation over pure TiO_2. This conjecture is in agreement with the results by Simakova et al.[18] In literature the formation of acetaldehyde was also observed in the absence of oxygen in the feed gas pointing to the participation of lattice oxygen in the oxidation reaction.[9] FTIR spectra showed that

ethanol adsorbs mainly dissociatively on TiO_2 according to results reported in literature.[5,21] Bands at 1049 and 1035 cm^{-1} were assigned to adsorption of ethoxy on Ti^{4+}. The bands are present in the spectra during reaction up to about 523 K, which is in good agreement with a Mars-van Krevelen mechanism for the high-temperature oxidation to acetaldehyde as was proposed by Li et al.[9] on Lewis acid sites on OMS-2.

As mentioned for TiO_2, acetaldehyde and H_2O were also detected in the TPD and decomposition experiments over the Au/TiO_2 ctalyst. Even though there is no direct evidence it seems reasonable to assume that their formation is also due to oxidation of ethanol involving lattice oxygen in addition to the dehydration and dehydrogenation reactions. In the co-feeding experiment the Au/TiO_2 catalyst is more active for acetaldehyde formation than bare TiO_2. For pure ZnO oxygen vacancies were identified as active sites in methanol synthesis.[35] Strunk et al.[36] showed in their study on the role of oxygen vacancies in methanol synthesis over Au/ZnO catalysts that high Au loadings lead to a large amount of oxygen vacancies on the catalyst surface, predominantly located at the Au perimeter.[36] Correspondingly, the presence of highly dispersed Au nanoparticles on TiO_2 leads to a higher reducibility of TiO_2 resulting in more oxygen vacancies than on bare TiO_2. Thus, oxygen vacancies on TiO_2 act as active sites (type II) for the high-temperature acetaldehyde formation following a Mars-van Krevelen mechanism. Thus, a higher reducibility of TiO_2 can be correlated with the activity for the high-temperature acetaldehyde formation. As was mentioned for bare TiO_2 this reaction is limited in the oxygen-free experiments because of the fixed reservoir of lattice oxygen.

The formation of CO_2 at high temperatures is due to total oxidation of ethanol and its intermediates formed during oxidation. The IR results obtained for ethanol oxidation over Au/TiO_2 show that during the formation of CO_2 at 473 K bands due to ethoxy and acetate species, acetaldehyde, and acetic acid are present on the surface. Thus, it can be assumed that such intermediate species are oxidized to CO_2 in agreement with earlier studies by Li et al.[9,10] Additionally, the formation of negligible amounts of acetic acid was observed in the co-feeding experiments as well as in the oxygen-free experiment over Au/TiO_2 at high temperatures (> 500 K). This observation supports the assumption that lattice oxygen participates in the reaction pathway pointing to a Mars-van Krevelen mechanism as observed for the acetaldehyde formation. In general, acetaldehyde is the first oxidation product and further oxidation leads to acetic acid formation.[37] Acetic acid formation was not observed over bare TiO_2, presumably because not enough active oxygen is available to oxidize acetaldehyde further. Contrary to our expectations no hint for enhanced acetic acid formation was found in the co-feeding experiment compared to the oxygen-free feed. The IR results indicate that small amounts of acetic acid remain strongly adsorbed on the catalyst surface in agreement with the results obtained by Li et al.[10]

During cooling lower yields and degrees of conversion were detected at temperatures below 500 K, and the low-temperature maximum was missing in a second experiment performed subsequently without any further pre-treatment. Low-temperature activity can be restored by oxidative pre-treatment before the oxidation experiment. Thus, the difference between heating and cooling experiments is due to catalyst deactivation by reversible poisoning as was observed already for methanol oxidation.[26] The presented FTIR results revealed that ethoxy species are consumed during reaction and new bands assigned to acetates, adsorbed acetaldehyde, acetic acid, gas-phase CO_2, and presumably carbonate species arise with increasing temperature. Changing the feed to inert He and subsequent switching to O_2/He led to a further decrease of the bands assigned to ethoxy species, and bands assigned to adsorbed acetaldehyde seem to increase slightly indicating the conversion of ethoxy to acetaldehyde in the presence of O_2. Also, CO_2 formation is only observed when O_2 is present. The bands assigned to acetate species and acetic acid remained stable even in O_2/He. Obviously, both species are strongly bound to the surface and not consumed during reaction. Thus, ethoxy is identified as reaction intermediate, while acetate species and acetic acid are catalyst poisons for the low-temperature acetaldehyde formation, which are strongly adsorbed at the Au perimeter atoms. In this way the active sites for the low-temperature reaction (active sites type I) are poisoned reversibly. The reaction mechanisms of ethanol conversion over Au/TiO_2 are illustrated in Scheme 1.

((Insert Scheme 1 here.))

Scheme 1. Proposed reaction scheme of the ethanol oxidation over Au/TiO_2. 1) Selective low-temperature oxidation to acetaldehyde and H_2O with active oxygen species O* (in close proximity to Au), occurring at active sites type I (Au perimeter); 2) selective high-temperature oxidation to acetaldehyde and H_2O at active sites type II (TiO_2) following a Mars-van Krevelen mechanism involving lattice oxygen; 3) selective oxidation to adsorbed acetates and H_2O; 4) re-filling of oxygen vacancies (□) by gas-phase oxygen. Total oxidation to CO_2 and H_2O is possible as side reaction from each intermediate.

Conclusions

Pure TiO_2 was found to be catalytically active above 500 K for the conversion of ethanol resulting in the selective oxidative dehydrogenation to acetaldehyde and water. To a minor extent total oxidation to CO_2 and H_2O was observed. The deposition of Au nanoparticles on TiO_2 resulted in a highly active bifunctional catalyst for the conversion of ethanol. The presence of highly dispersed Au nanoparticles induced the additional selective oxidation to acetaldehyde at temperatures below 400 K, whereas the selective oxidation to acetaldehyde at higher temperatures above 475 K was also observed on pure TiO_2. Therefore, selective low-temperature oxidation is assumed to occur at the perimeter of the Au nanoparticles (active sites type I), which are considered essential for activating O_2. For the high-temperature oxidation a second type of active sites is identified located on TiO_2 (type II), and the oxidative dehydrogenation to acetaldehyde follows most likely

a Mars-van Krevelen mechanism. The total oxidation to CO_2 and H_2O is catalyzed by Au/TiO_2 as well, but still to a minor extent. Negligible amounts of acetic acid were identified as second oxidation product at high temperatures also formed according to a Mars-van Krevelen mechanism. Ethoxy species detected by IR spectroscopy are identified as reactive intermediates in ethanol conversion, whereas strongly bound acetates and presumably acetic acid were found to act as reversible catalyst poisons for the selective low-temperature oxidation route, but not for the high-temperature route. The presence of Au nanoparticles also enhanced the high-temperature oxidation pathway on TiO_2 based on an enhanced reducibility of TiO_2. Therefore, metal-support interactions play a decisive role in the oxidation of ethanol over Au/TiO_2.

Acknowledgements

The authors gratefully acknowledge the financial support by the Deutsche Forschungsgemeinschaft (DFG) within the collaborative research centre (SFB 558) "Metal-Substrate Interactions in Heterogeneous Catalysis".

Notes and references

[a]Laboratory of Industrial Chemistry, Ruhr-University Bochum, Universitätsstr. 150, 44801 Bochum, Fax: +49(0)23432-14115, E-mail: muhler@techem.rub.de

1 C. Lamy, E. Belgsir, J.-M. Léger, *J. Appl. Electrochem.*, 2001, **31**, 799.
2 S. Song, P. Tsiakaras, *Appl. Catal. B: Environ.*, 2006, **63**, 187.
3 M. Kamarudin, S. Kamarudin, M. Masdar, W. Daud, *Int. J. Hydrogen Energ.*, 2012.
4 A. Erdőhelyi, J. Raskó, T. Kecskés, M. Tóth, M. Dömök, K. Baán, *Catal. Today*, 2006, **116**, 367.
5 J. Raskó, A. Hancz, A. Erdőhelyi, *Appl. Catal. A: Gen.*, 2004, **269**, 13.
6 S. M. de Lima, A. M. da Silva, L. O. da Costa, U. M. Graham, G. Jacobs, B. H. Davis, L. V. Mattos, F. B. Noronha, *J. Catal.*, 2009, **268**, 268.
7 G. Carotenuto, A. Kumar, J. Miller, A. Mukasyan, E. Santacesaria, E. Wolf, *Catal. Today*, 2013, **203**, 163.
8 L. Petkovic, S. N. Rashkeev, D. Ginosar, *Catal. Today*, 2009, **147**, 107.
9 J. Li, R. Wang, J. Hao, *J. Phys. Chem. C*, 2010, **114**, 10544.
10 H. Li, G. Qi, Tana, X. Zhang, X. Huang, W. Li, W. Shen, *Appl. Catal. B: Environ.*, 2011, **103**, 54.
11 M. Baerns, A. Behr, J. Gmehling, H. Hofmann, U. Onken, A. Renken (Eds.) *Technische Chemie*, Wiley-VCH, Weinheim, 2006.
12 A. P. V. Soares, M. F. Portela, A. Kiennemann, *Catal. Rev.*, 2005, **47**, 125.
13 *Ullmann's Encyclopedia of Industrial Chemistry*, Wiley-VCH, Weinheim.
14 R. Lin, M.-f. Luo, Q. Xin, G.-Q. Sun, *Catal. Lett.*, 2004, **93**, 139.
15 G. A. M. Hussein, N. Sheppard, M. I. Zaki, R. B. Fahim, *J. Chem. Soc. Faraday Trans.*, 1991, **87**, 2661.
16 W. Zhang, S. Oyaman, W. Holstein, *Catal. Lett.*, 1996, **39**, 67.
17 V. I. Sobolev, K. Y. Koltunov, O. A. Simakova, A.-R. Leino, D. Y. Murzin, *Appl. Catal. A: Gen.*, 2012, **433-434**, 88.
18 O. A. Simakova, V. I. Sobolev, K. Y. Koltunov, B. Campo, A.-R. Leino, K. Kordás, D. Y. Murzin, *ChemCatChem*, 2010, **2**, 1535.
19 V. I. Sobolev, O. A. Simakova, K. Y. Koltunov, *ChemCatChem*, 2011, **3**, 1422.
20 B. Kilos, A. T. Bell, E. Iglesia, *J. Phys. Chem.*, 2009, **113**, 2830.
21 W.-C. Wu, C.-C. Chuang, J.-L. Lin, *J. Phys. Chem. B*, 2000, **104**, 8719.
22 L. Óvári, F. Solymosi, *Langmuir*, 2002, **18**, 8829.
23 M. C. Holz, K. Kähler, K. Tölle, A. C. van Veen, M. Muhler, *Phys. Status Solidi B*, 2013, **250**, 1094.
24 S. Oyama, W. Zhang, *J. Am. Chem. Soc*, 1996, **118**, 7173.
25 J. Gao, A. V. Teplyakov, *J. Catal.*, 2013, **300**, 163.
26 K. Kähler, M. C. Holz, M. Rohe, A. van Veen, M. Muhler, *J. Catal.*, 2013, **299**, 162.
27 G. A. M. Hussein, N. Sheppard, M. I. Zaki, R. B. Fahim, *J. Chem. Soc. Faraday Trans.*, 1989, **85**, 1723.
28 G. Mul, A. Zwijnenburg, B. van der Linden, M. Makkee, J. A. Mouljin, *J. Catal.*, 2001, **201**, 128.
29 W. Rachmady, M. A. Vannice, *J. Catal.*, 2002, **207**, 317.
30 M. El-Maazawi, A. Finken, A. Nair, V. Grassian, *J. Catal.*, 2000, **191**, 138.
31 L.-F. Liao, W.-C. Wu, C.-Y. Chen, J.-L. Lin, *J. Phys. Chem. B*, 2001, **105**, 7678.
32 C.-C. Chuang, W.-C. Wu, M.-C. Huang, I.-C. Huang, J.-L. Lin, *J. Catal.*, 1999, **185**, 423.
33 M. A. Henderson, *J. Phys. Chem. B*, 1997, **101**, 221.
34 M. Farnesi Camellone, J. Zhao, L. Jin, Y. Wang, M. Muhler, D. Marx, *Angew. Chem. Int. Ed*, 2013, **52**, 5780.
35 J. Strunk, K. Kähler, X. Xia, M. Muhler, *Surf. Sci.*, 2009, **603**, 1776.
36 J. Strunk, K. Kähler, X. Xia, M. Comotti, F. Schüth, T. Reinecke, M. Muhler, *Appl. Catal. A: Gen.*, 2009, **359**, 121.
37 S. E. Davis, M. S. Ide, R. J. Davis, *Green Chem.*, 2013, **15**, 17.

Journal Name

RSCPublishing

ARTICLE

Figures: All single column figures except scheme 1(double column size).

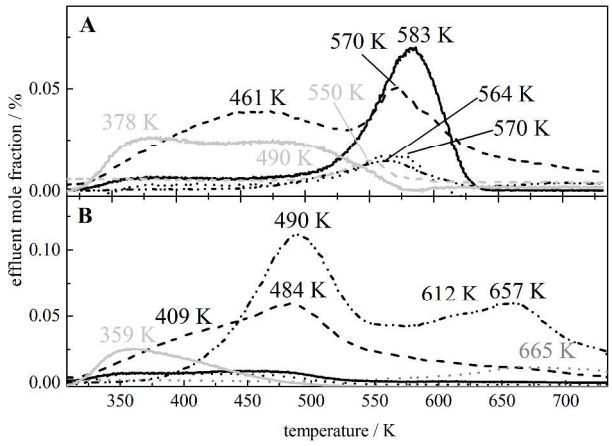

Figure 1 QMS traces of the ethanol TPD experiments with A) TiO_2 and B) Au/TiO_2 displaying the effluent mole fractions of CH_3CH_2OH (▬), H_2O (– – –), $CH_2{=}CH_2$ (▬), CH_3CHO (▪▪▪), H_2 (□ ▪ ▪), $(C_2H_5)_2O$ (– – –), and CO_2 (▪▪▪). The heating rate was 3 K min^{-1}.

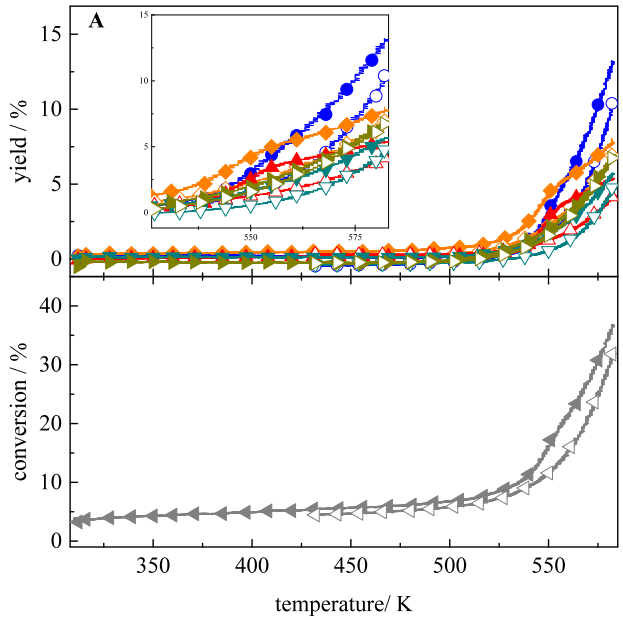

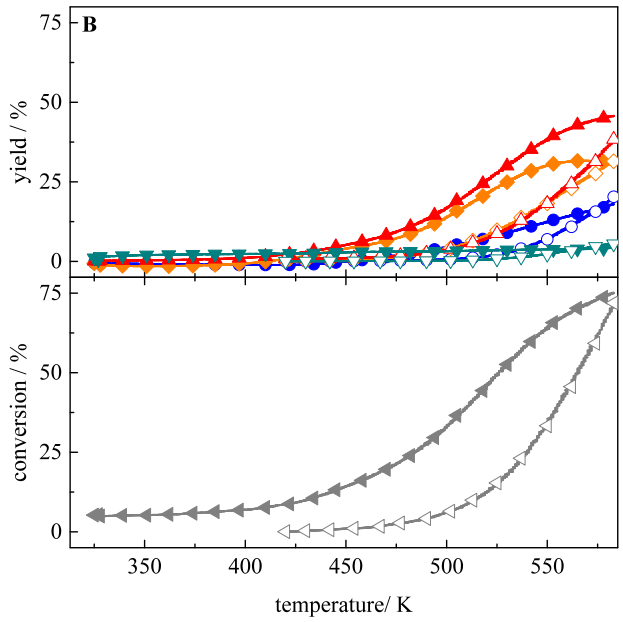

Figure 2 Conversion and yields during ethanol decomposition over (A) TiO_2 and (B) Au/TiO_2 after O_2 pre-treatment at 573 K. Conversion of CH_3CH_2OH (◄) and yields of H_2 (▲, □), H_2O (●, □), CH_3CHO (♦, □), $CH_2{=}CH_2$ (▼, □), and $(C_2H_5)_2O$ (►, □) are shown. Traces with full symbols were obtained during heating, traces with open symbols during cooling of the catalyst.

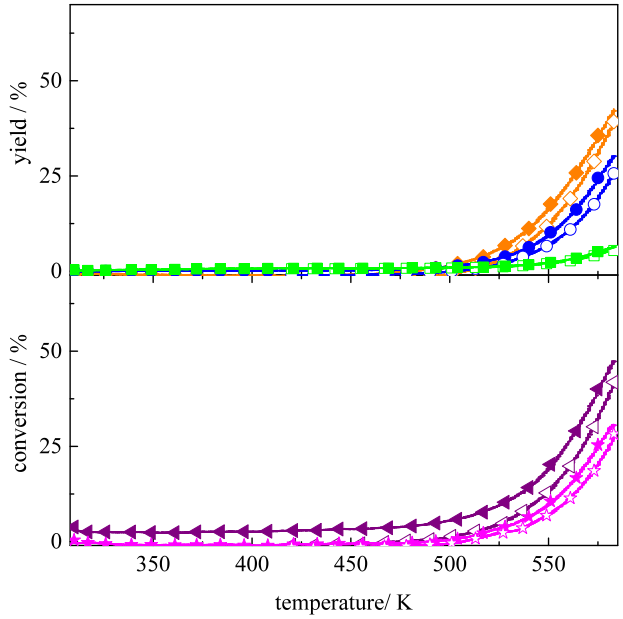

Figure 3: Conversion and yields during ethanol oxidation over TiO_2 after O_2 pre-treatment at 573 K. Conversion of CH_3CH_2OH (◄, □) and O_2 (★, □) and yields of H_2O (●, □), CO_2 (■, □), and CH_3CHO (♦, □) are shown. Traces with full symbols were obtained during heating, traces with open symbols during cooling of the catalyst.

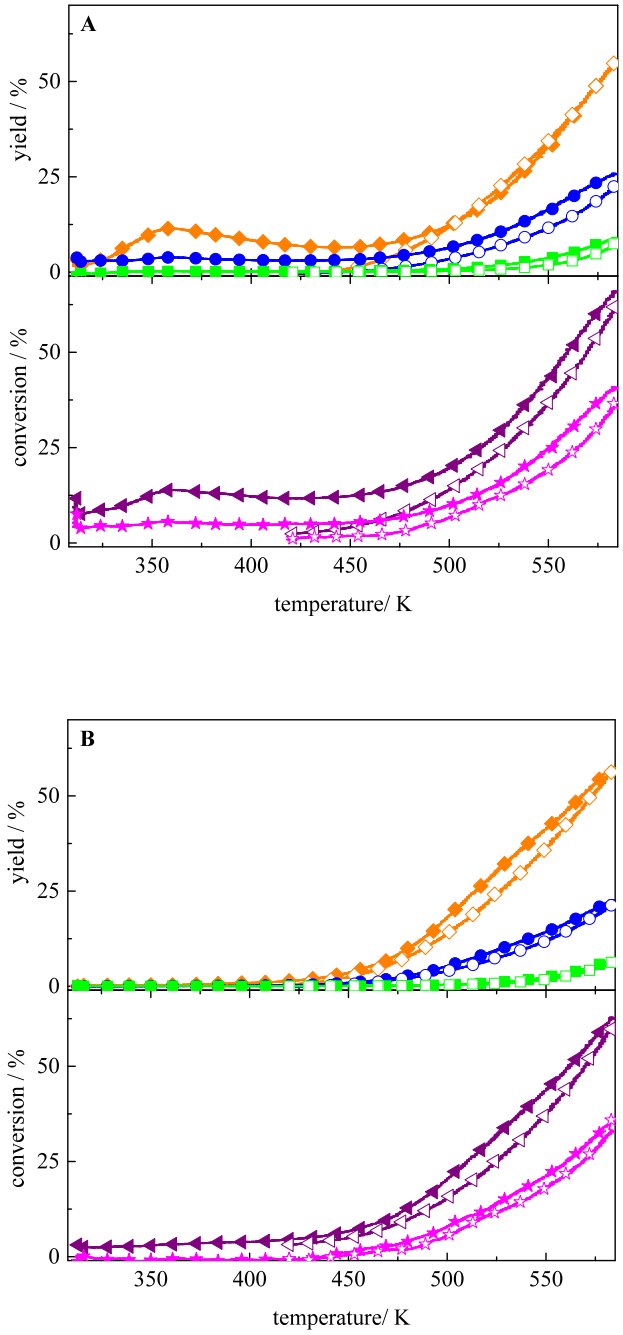

Figure 4 Conversion and yields during ethanol oxidation over Au/TiO_2 after O_2 pre-treatment at 573 K (A: 1st run, B: 2nd run). Conversion of CH_3CH_2OH (◀, □) and O_2 (★, □) and yields of H_2O (●, □), CO_2 (■, □), and CH_3CHO (♦, □) are shown. Traces with full symbols are obtained during heating, traces with open symbols during cooling of the catalyst.

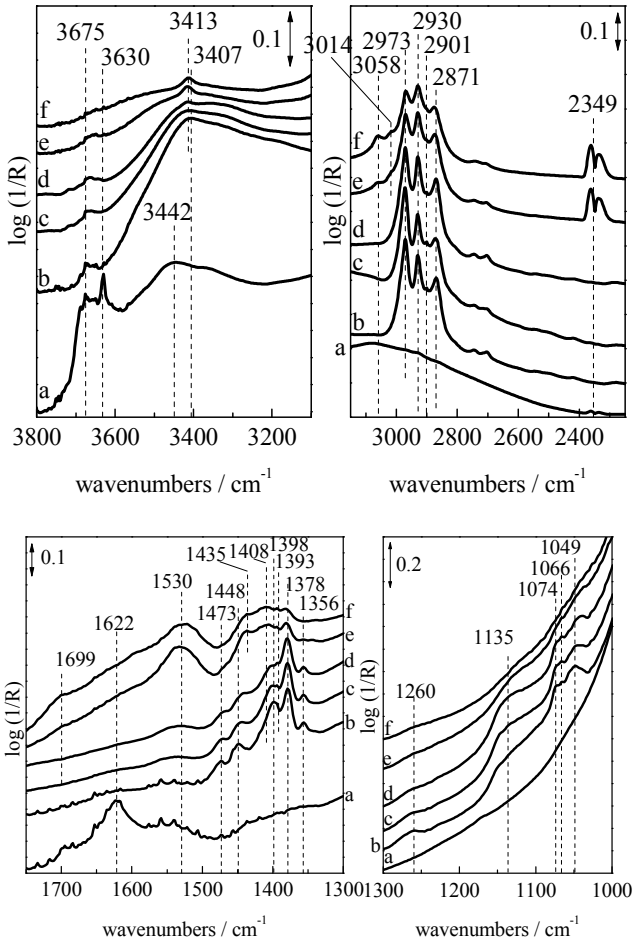

Figure 5 DRIFT spectra detected during ethanol oxidation over of Au/TiO_2 after oxidative pre-treatment: (a) at 303 K in He after pre-treatment in O_2/He at 573 K; in 0.39% CH_3CH_2OH/ 0.39% O_2/ He at (b) 303 K, (c) 373 K, (d) 423 K, (e) 523 K, and (f) 573 K.

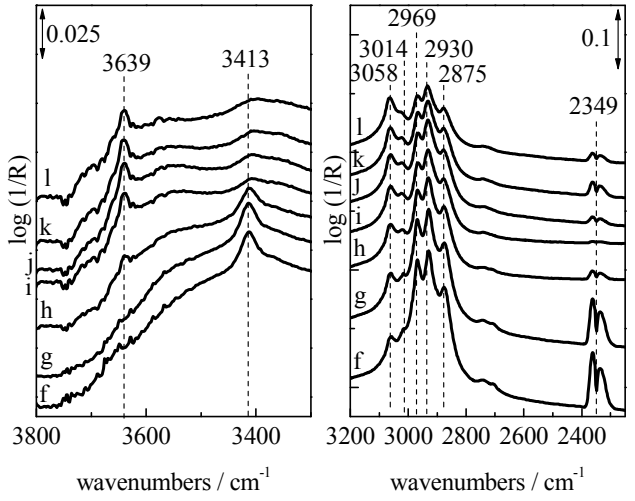

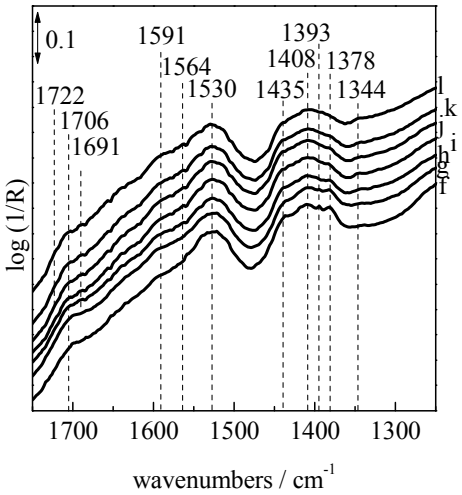

Figure 6 DRIFT spectra of Au/TiO_2: (f) in 0.39% CH_3CH_2OH/ 0.39% O_2/ He at 573 K, in He at 573 K for (g) 1 min, (h) 5 min, (i) 29 min, and in 0.39% O_2/ He for (j) 1 min, (k) 5 min, and (l) 29 min.

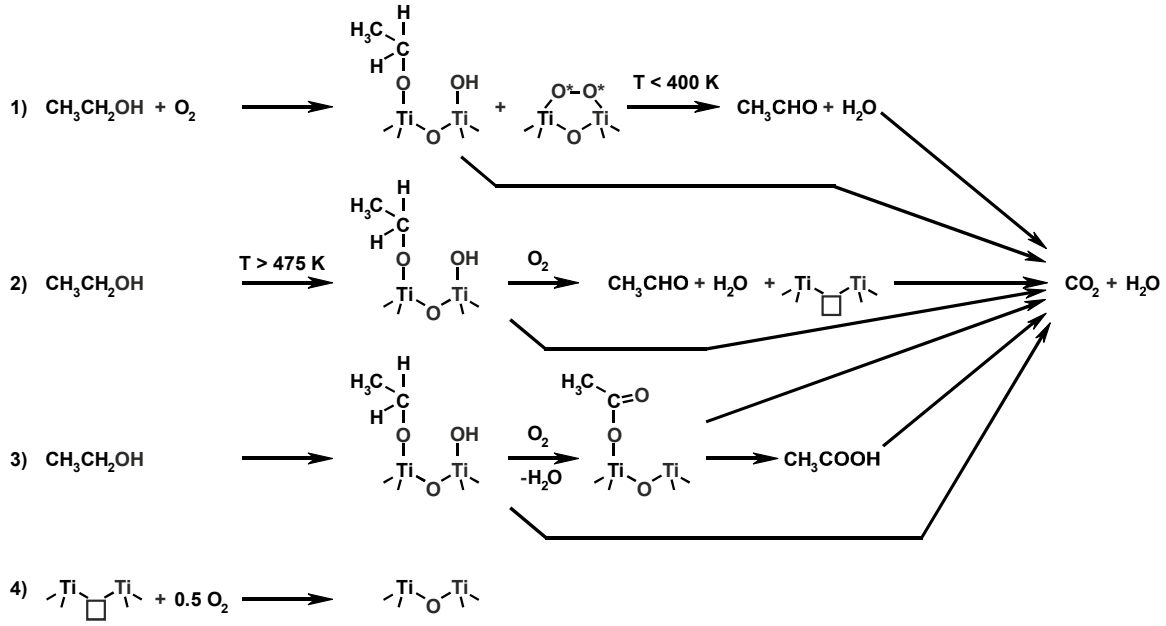

Scheme 1 Proposed reaction scheme of ethanol oxidation over Au/TiO_2. 1) Selective low-temperature oxidation to acetaldehyde and H_2O with active oxygen species O* (in close proximity to Au), occurring at active sites type I (Au perimeter); 2) selective high-temperature oxidation to acetaldehyde and H_2O at active sites type II (TiO_2) following a Mars-van Krevelen mechanism involving lattice oxygen; 3) selective oxidation to adsorbed acetates and H_2O; 4) re-filling of oxygen vacancies ( ) by gas-phase oxygen. Total oxidation to CO_2 and H_2O is possible as side reaction from each intermediate.